AIP | Review of Scientific Instruments

Investigation on target normal sheath acceleration through measurements of ions energy distribution

S. Tudisco, C. Altana, G. Lanzalone, A. Muoio, G. A. P. Cirrone, D. Mascali, F. Schillaci, F. Brandi, G. Cristoforetti, P. Ferrara, L. Fulgentini, P. Koester, L. Labate, D. Palla, and L. A. Gizzi

Citation: Review of Scientific Instruments **87**, 02A909 (2016); doi: 10.1063/1.4934691
View online: http://dx.doi.org/10.1063/1.4934691
View Table of Contents: http://scitation.aip.org/content/aip/journal/rsi/87/2?ver=pdfcov
Published by the AIP Publishing

Investigation on target normal sheath acceleration through measurements of ions energy distribution

S. Tudisco,[1,a)] C. Altana,[1,2] G. Lanzalone,[1,3] A. Muoio,[1,4] G. A. P. Cirrone,[1] D. Mascali,[1] F. Schillaci,[1] F. Brandi,[5,6] G. Cristoforetti,[5] P. Ferrara,[5] L. Fulgentini,[5] P. Koester,[5] L. Labate,[5,7] D. Palla,[5,7,8] and L. A. Gizzi[5,7]

[1]*Istituto Nazionale di Fisica Nucleare, Laboratori Nazionali del Sud, Via S. Sofia 62, 95123 Catania, Italy*
[2]*Dipartimento di Fisica e Astronomia, Università degli Studi di Catania, Via S. Sofia 64, 95123 Catania, Italy*
[3]*Università degli Studi di Enna "Kore," Via delle Olimpiadi, 94100 Enna, Italy*
[4]*Dipartimento di Fisica e Scienze della Terra, Università degli Studi di Messina, Viale F.S. D'Alcontres 31, 98166 Messina, Italy*
[5]*Consiglio Nazionale delle Ricerche, Istituto Nazionale di Ottica, Intense Laser Irradiation Laboratory, Via G. Moruzzi 1, 56124 Pisa, Italy*
[6]*Istituto Italiano di Tecnologia, Via Morego 30, 16163 Genova, Italy*
[7]*Istituto Nazionale di Fisica Nucleare, Sezione di Pisa, Largo B. Pontecorvo 3, 56127 Pisa, Italy*
[8]*Dipartimento di Fisica, Università di Pisa, Largo B. Pontecorvo 3, 56127 Pisa, Italy*

(Presented 24 August 2015; received 21 August 2015; accepted 13 October 2015; published online 6 November 2015)

An experimental campaign aiming at investigating the ion acceleration mechanisms through laser-matter interaction in femtosecond domain has been carried out at the Intense Laser Irradiation Laboratory facility with a laser intensity of up to 2×10^{19} W/cm^2. A Thomson parabola spectrometer was used to obtain the spectra of the ions of the different species accelerated. Here, we show the energy spectra of light-ions and we discuss their dependence on structural characteristics of the target and the role of surface and target bulk in the acceleration process. © *2015 AIP Publishing LLC.* [http://dx.doi.org/10.1063/1.4934691]

I. INTRODUCTION

In recent years, laser ion acceleration has gained much interest focusing on fast ions emitted from a solid target by intense laser irradiation.[1,2] Protons and heavier ions can be accelerated up to tens MeV per nucleon via various mechanisms such as target normal sheath acceleration (TNSA),[3–5] radiation pressure acceleration (RPA),[6–10] and break-out afterburner acceleration (BOA).[11–13]

Our work concerns the TNSA regime, in which an intense laser pulse is focused (>10^{18} W/cm^2) on a 10 micrometers thick foil target. Several processes involving energy transfer between the laser pulse and the target electrons occur, with a significant role played by plasma density gradient set up by the specific laser pulse temporal properties due to Amplified Spontaneous Emission (ASE) and to laser pulse compression. Consequently, a population of hot electrons with a mean free path larger than the target thickness is produced. Hence, these electrons can cross the target itself, often subject to strong magnetic fields with complex features depending upon target properties,[14,15] setting up an intense electrostatic field due to the charge imbalance between positive ions at rest in the target and the expanding electron sheath.[16]

Typically, this field accelerates simultaneously several ion species, originated partly from the bulk target material, but predominantly from the hydrocarbon contaminant layers present on both sides of the target foils. Therefore, such ion sources are typically multi-species (protons, several charge states of carbon, and the bulk target elements) and demand spectrometers with adequate charged species discrimination capability. Detecting and identifying the energy spectra of individual ion species are the key for understanding the underlying acceleration mechanism. In this context, we carried out a systematic experimental investigation to identify the role of target properties in TNSA, with special attention to target thickness and dielectric properties. We used a full range of ion, optical, and X-ray diagnostics to investigate laser-plasma interaction and ion acceleration. We focus on the results obtained using a Thomson Parabola Spectrometer (TPS).

In the TPS, often used in such experiments, ions with different charge-to-mass ratios are separated into distinct parabolas. This allows to extract information for each ion species when several ions are generated simultaneously in a given solid angle.

In this paper, we discuss the energy spectra of light-ions depending on structural characteristics of the target.

II. EXPERIMENTAL SETUP

TPS has been employed to characterize ion beams produced in TNSA regime. The working principle, widely described in the literature,[17–20] is based on parallel electric and magnetic fields acting on a sharply collimated ion beam propagating orthogonally to the fields themselves. The Lorentz force splits the different ion species according to their

Note: Contributed paper, published as part of the Proceedings of the 16th International Conference on Ion Sources, New York, New York, USA, August 2015.

a)Author to whom correspondence should be addressed. Electronic mail: tudisco@lns.infn.it.

charge-to-mass ratio and energy. This result in a series of parabolic traces on the detector, each of them corresponding to well determined ion species.

Our TPS is housed in a vacuum chamber, operating at a pressure of 10^{-6} Torr, and differentially pumped with respect to the target chamber. Ions enter the TPS through a collimator consisting of two pinholes. The first pinhole is 1 mm in diameter, drilled in a 2 cm thick substrate consisting of a double layer matrix of brass and lead in order to collimate the ions beam and to shield the detector from γ- and X-rays. The second pinhole is 100 μm in diameter, drilled in a 1 mm thick aluminum layer and is responsible for the spatial and energy resolution of the spectrometer. The pinhole separation is 10 cm. After the collimator, ions enter a deflection sector consisting of parallel electric and magnetic field partially overlapping with each other. After passing the drift region, which allows the particles to increase deflection and separation among different traces, the ion position is detected using an imaging system. In our case, a micro-channel plate coupled to a phosphor screen 75 mm in diameter (MCP-PH) and an EMCCD camera are used to observe online the spectrogram in single shot measurements. Further details of the TPS are given elsewhere.[21,22]

The experiments have been performed at the Intense Laser Irradiation Laboratory (ILIL) in Pisa where a Ti:sapphire laser system is operating, which delivers 40 fs–800 nm pulses with energy on target up to 400 mJ. The ILIL laser pulse exhibits an ASE contrast greater than 10^9 and a ps contrast $>10^7$ at 10 ps before the peak pulse. The beam is focused on the target at an angle of incidence of 15° using an off-axis parabolic mirror; the corresponding maximum intensity on target was up to 2×10^{19} W/cm^2. The target was mounted on a three-axis translational stage system at the center of a 640 mm diameter interaction chamber. Targets consisting of different materials were used. Here, we focus on deuterated plastic(CD_2) foil targets of 10 μm thickness.

TPS was placed in the direction of the target normal, with a distance of 129 cm from the target surface to MCP-PH, as shown in Fig. 1.

III. DATA ANALYSIS

The data analysis provides an estimate of ion energy distribution and temperature. By means of TPS calibration, it is possible to determine the kinetic energy of different ions

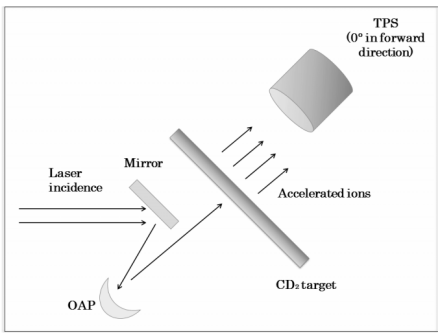

FIG. 1. Sketch of the experimental setup.

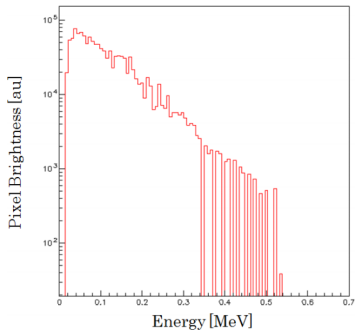

FIG. 2. Proton spectrum obtained by means of magnetic field.

(protons and deuterons) distributed along the parabolas and therefore reconstruct the whole spectrum.[23]

Fig. 2 shows as an example the spectrum of proton energy obtained with a CD_2 target: the trend of the MCP brightness is shown as a function of the ion's kinetic energy obtained by means of magnetic deflection. The brightness of the traces is correlated with the number of particles.

Assuming a Maxwell-Boltzmann distribution for the ions energy, the theoretical curve is given by the following equation:[24]

$$J(E) = C(E) \exp\left(-\frac{E}{kT}\right). \quad (1)$$

By fitting the spectra with Eq. (1), one can calculate the ion temperature. Then, the coefficient C of the fit gives information related to the total number of ions.

IV. RESULTS AND DISCUSSION

Fig. 3 shows an image of the phosphor screen of the MCP from a laser shot onto a 10 μm thick CD_2 foil. The image shows parabolas from protons and deuterons. The bright spot in the lower left corner is due to γ and X-ray radiation and to neutral particles moving straight through the electromagnetic field. The parabolas show a sharp cutoff near the origin, which corresponds to the maximum ion energies.

The measurements were carried out at different laser focusing conditions by moving the translation stage of the target. Here, we focus the attention on ions temperature and total number as function of the position of the target foil along the focusing axis.

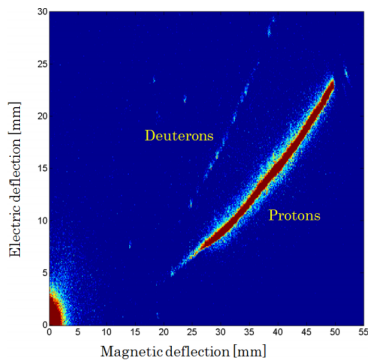

FIG. 3. Spectrograms from a 10 μm thick CD_2 target.

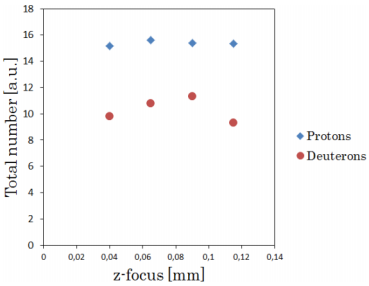

FIG. 4. Total number of protons and deuterons as function of the focal spots.

The number of protons is much higher than the number of heavy deuterons, as shown in the plot of Fig. 4, although the target was made of bulk CD_2.

The protons result from the hydrocarbon contamination on the rear target surface. The above observation confirms that surface ion contribution is dominant with respect to volume contribution, as shown schematically in Fig. 5. It is possible that the protons are accelerated first and shield the heavier ions from electric field, coming later.

After the retrieval of the protons and deuterons spectra, the temperature of the distribution was calculated. Fig. 6 shows the temperature as a function of the focal position showing that protons and deuterons temperatures exhibit an opposite trend: protons exhibit a maximum corresponding to the best focus where deuterons show a minimum temperature. These preliminary observations clearly show that ion acceleration originates from a complex scenario set by the laser-target interaction conditions. Detailed modeling is currently being carried out to unfold the origin of surface and volume acceleration processes observed here, taking into account the laser target interaction mechanisms as emerging from other measurements including optical and X-ray spectroscopies and optical transition radiation imaging.

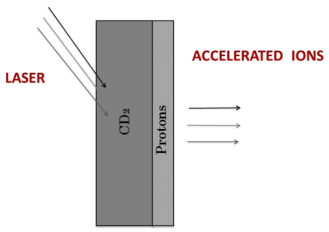

FIG. 5. Schematic representation of surface and volume emission.

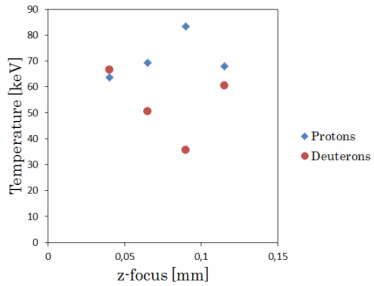

FIG. 6. Temperature of protons (blue diamond) and deuterons (red circle) as function of focus.

V. CONCLUSIONS

Ion acceleration mechanism in TNSA regime was here investigated by using a Thomson Parabola spectrometer. Surface and volume contributions to the ion acceleration have been clearly identified by using a unique target configuration consisting of a thin CD_2 foil. Preliminary results show that protons and deuterons temperatures show opposite trend, suggesting a complex interplay between surface and volume acceleration. A detailed analysis of these results is currently in progress, also in view of the full set of measurements of laser-plasma interaction and laser-pulse specifications.

[1]E. L. Clark *et al.*, Phys. Rev. Lett. **85**, 1654 (2000).
[2]O. M. Hegelich *et al.*, Phys. Rev. Lett. **85**, 085002 (2002).
[3]A. Macchi *et al.*, Rev. Mod. Phys. **85**, 751 (2013).
[4]J. Fuchs *et al.*, Nat. Phys. **2**, 48 (2006); L. Robson *et al.*, *ibid.* **3**, 58 (2007).
[5]M. Passoni *et al.*, New J. Phys. **12**, 045012 (2010).
[6]T. Esirkepov *et al.*, Phys. Rev. Lett. **92**, 175003 (2004).
[7]A. P. L. Robinson *et al.*, New J. Phys. **10**, 013021 (2008).
[8]A. P. L. Robinson *et al.*, Plasma Phys. Control. Fusion **51**, 024004 (2009).
[9]A. Macchi *et al.*, New J. Phys. **12**, 045013 (2010).
[10]B. Qiao *et al.*, Phys. Rev. Lett. **108**, 115002 (2012); S. Kar *et al.*, *ibid.* **109**, 185006 (2012).
[11]L. Yin *et al.*, Laser Part. Beams **24**, 291–298 (2006).
[12]L. Yin *et al.*, Phys. Rev. Lett. **107**, 045003 (2011).
[13]L. A. Gizzi *et al.*, Phys. Rev. Spec. Top.–Accel. Beams **14**, 011301 (2011).
[14]T. Ceccotti *et al.*, Phys. Rev. Lett. **111**, 185001 (2013).
[15]D. Jung *et al.*, Phys. Rev. Lett. **107**, 115002 (2011).
[16]M. Passoni *et al.*, Rev. Sci. Instrum. **55**, 1229 (1984).
[17]K. Harres *et al.*, Rev. Sci. Instrum. **79**, 093306 (2008).
[18]D. Jung *et al.*, Rev. Sci. Instrum. **82**, 013306 (2011).
[19]J. A. Cobble *et al.*, Rev. Sci. Instrum. **82**, 113504 (2011).
[20]R. F. Schneider *et al.*, J. Appl. Phys. **57**, 1 (1985).
[21]G. A. P. Cirrone *et al.*, Radiat. Eff. Defects Solids **165**, 767 (2010).
[22]M. Maggiore *et al.*, Acta Tech. CSAV **56**, 739 (2011).
[23]F. Schillaci *et al.*, J. Instrum. **9**, T10003 (2014).
[24]I. H. Hutchinson, *Principles of Plasma Diagnostics* (Cambridge University Press, Cambridge, 1987).